Mem. SR Center Ritsumeikan Univ. No. 23, 3-8 (2021)

Chemical State Analysis on Ni Species Supported on Carbon During Electrochemical Reduction Process

Takaya Ishida[1], Takuya Tsuji[1], Hirona Yamagishi[2], Yusaku Yamamoto[1], Misaki Katayama[2], and Yasuhiro Inada[1,2]

1) *Department of Applied Chemistry, College of Life Sciences, Ritsumeikan University, 1-1-1 NojiHigashi, Kusatsu 525-8577, Japan*
2) *The SR Center, Ritsumeikan University, 1-1-1 Noji-Higashi, Kusatsu 525-8577, Japan*

Initial electrochemical reduction mechanism of NiO supported on acetylene black (NiO/AB) has been analyzed by the X-ray absorption fine structure (XAFS) measurements. The extended X-ray absorption fine structure analysis has revealed that the particle size of the Ni species becomes small during the conversion from NiO to Ni(0) at the first reduction process, which is accompanied by the formation of Li_2CO_3. The X-ray absorption near edge structure analysis at the O K-edge has clarified that the formation of Li_2CO_3 is started below 1 V using Li counter electrode, suggesting the decomposition of electrolyte solvent. The reduction of NiO takes place after a certain amount of reduction current has flowed. The XAFS analysis in this study supports that ionic compounds containing Li^+ is necessary for the reduction of NiO in order to receive the oxide ions from NiO.

1. Introduction

Lithium-ion batteries (LIBs) are a useful device for electric power storage and are widely used in familiar devices such as mobile phones and laptop computers. However, the LIB performance needs to be improved for use in electric vehicles and renewable energy storage. The enlargement of the battery capacity is one of the important requirements, and the electrode design based on a new electrochemical reaction for the rechargeable battery is an urgent problem of modern society.

The performance of graphite carbon is excellent as a negative electrode material for LIBs. However, its capacity is not sufficient for applications of next-generation battery [1]. The investigations are conducted with the aim of developing a battery system, which uses a conversion reaction for the negative electrode as a next-generation LIB with higher capacity [2]. In the case of the negative electrode, the insertion/desertion reaction of lithium ions into/from graphite accompanied by the redox reaction of lithium, equation (1), shows the theoretical capacity of 372 mA h g^{-1} [3].

$$Li^+ + C_6 + e^- \rightleftharpoons LiC_6 \qquad (1)$$

Instead of the Li^+/Li pair, the redox conversion of transition metal oxides (MO_x: M = Fe, Co, Ni, Cu, etc.) is a candidate for the alternative of the active material, because the conversion reaction of MO_x can use multi electrons per an M atom although the redox potential is relatively high. The conversion reaction of MO_x is formally expressed by equation (2), and the theoretical capacity is calculated to be 718 mA h g^{-1} in the case of NiO [1].

$$NiO + 2e^- \rightleftharpoons Ni + O^{2-} \qquad (2)$$

When Li^+ is existed in the system, the produced oxide ion is stabilized by forming Li_2O as represented by equation (3) [1].

$$NiO + 2Li^+ + 2e^- \rightleftharpoons Ni + Li_2O \qquad (3)$$

Although this conversion reaction is promising in terms of achieving the high capacity as the negative electrode of LIBs, there are still some problems for the practical application of NiO, such as the potential polarization between the charge and discharge process and the poor cycle property [4]. It has been reported that the particle size is a key factor to achieve good reversibility [5] and that the modification of the conductive additive improves the electrode performance [6]. Furthermore, it is well known that an unexpectedly high irreversible capacity appears at the first reduction process of NiO to generate the Ni(0) species, and the capacity is not recovered by the next oxidation process to regenerate NiO. The excess current is believed to use to form a so-called solid electrolyte interphase (SEI), in which the elements of Li, C, O, and F are contained in the form of LiF, Li_2CO_3, alkyl carbonate lithium, etc. [7-9].

Although the component of SEI has been evaluated and it is known that the formation of SEI contributes to prevent the further decomposition of electrolyte solvent [10], the chemical state change of the Ni species during the first reduction process together with the SEI formation is still unclear. The microscopic picture and the formation mechanism of the reduced Ni species existed in SEI are necessary knowledge to achieve a good reversibility of succeeding conversion processes between Ni(0) and NiO. In this study, we have thus analyzed the chemical state change of the Ni species during the first reduction process of NiO supported on carbon by the Ni K- and L-edge X-ray absorption fine structure (XAFS) measurements. In addition, the O K-edge XAFS measurements have been carried out to gain insight into the components of SEI.

2. Experimental

The powder of NiO supported on acetylene black (NiO/AB) was prepared by the conventional impregnation method. The AB powder was added in an aqueous solution of $Ni(NO_3)_2 \cdot 6H_2O$, and the mixture was dried for 72 h at 70 °C. Then, it was calcined in air for 1 h at 300 °C. The actual Ni loading of NiO/AB was determined to be 44 wt% by thermogravimetry. A mixture slurry of the synthesized NiO/AB powder and a solution of binder polymer (polyvinylidene difluoride: PVDF) was applied on a Cu foil as the current collector to prepare the NiO/AB electrode sheet. The mass ratio of NiO/AB and PVDF was 6:4.

The electrochemical cell was assembled using the NiO/AB electrode, a Li foil as the counter electrode, two porous polypropylene films as the separator, and 1 mol dm^{-3} $LiPF_6$ solution dissolved in a mixture of ethylene carbonate and diethyl carbonate. Because the NiO/AB electrode was operated with respect to the Li counter electrode, the discharge operation corresponds to the reduction process of NiO. The electrochemical cell was discharged and stopped at various capacities. Then, the cell was disassembled in a glove box filled with Ar, and the electrode was taken out for all XAFS measurements.

The Ni K-edge XAFS measurements were performed at BL-3 of the SR Center (Ritsumeikan University) and BL-9C of Photon Factory (High energy Accelerator Research Organization) in the transmission mode. The Ni $L_{2,3}$-edge and O K-edge XANES measurements were carried out at BL-11 of the SR Center in the modes of the partial electron yield (PEY), the total electron yield (TEY), and the partial fluorescence yield (PFY).

3. Results and Discussion

The charge and discharge curves of the electrochemical cell with the NiO/AB electrode are shown in Fig. 1. The first discharge capacity was 899 mA h g^{-1}, and the succeeding charge capacity was 459 mA h g^{-1}, thus there was the irreversible capacity of 440 mA h g^{-1} for the first cycle, suggesting the existence of the reduction reaction other than the reduction of NiO. The formation of SEI in the NiO/AB electrode was proposed as one of the possible reactions [11,12]. In contrast, there was no irreversible capacity in the second cycle, and the observed capacities are approximately 480 mA h g^{-1}, which is consistent with the theoretical capacity of the NiO/AB electrode with the NiO loading of 44 wt%. The discharge/charge reaction proceeds reversibly on and after the second cycle.

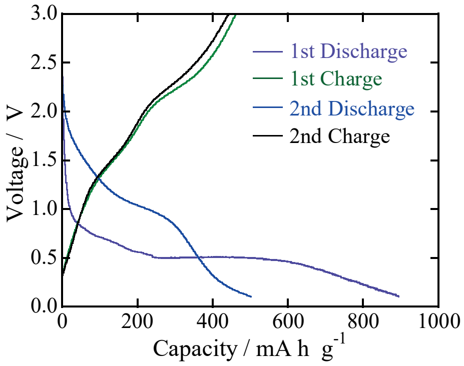

Fig. 1 The charge and discharge curves during the first and second cycles of the electrochemical cell with the NiO/AB electrode at the constant current rate of 0.5 C. The cell voltage was limited between 3.0 V and 0.1 V.

The results of the Ni K-edge XAFS measurements are summarized in Fig. 2 for the NiO/AB electrodes disassembled at various states during the first discharge process. The initial X-ray absorption near edge structure (XANES) spectrum was consistent with that of NiO. The X-ray absorbance at the white line peak was decreased and the lower shift was observed for the edge energy during the progress of the discharge process. Finally, the edge energy was reached to that of Ni foil after the discharge operation up to 0.1 V vs. Li^+/Li, whereas the shape of the XANES spectrum was slightly different from that of Ni foil. The double peak structure just above the absorption edge seems to be flattened for the Ni/AB electrode, and the difference will be discussed later.

The composition of the Ni species was determined by the linear combination fitting of the observed XANES spectrum using the reference spectra of NiO and Ni(0). As mentioned above and discussed later, because the final XANES spectrum was slightly different from that of Ni foil, the final spectrum observed for the reduction process was used as the reference of Ni(0). Similarly, the observed initial spectrum was used as the reference for NiO. The composition change is plotted in Fig. 2(B) as a function of the reduction (discharge) capacity. It has been clarified that a trace amount of NiO is reduced up to 300 mA h g^{-1}, and then the reduction of NiO is facilitated in the region of discharge capacity larger than 300 mA h g^{-1}. The final discharge capacity at 0.1 V vs. Li^+/Li was *ca.* 900 mA h g^{-1} (see Fig. 1) and was extremely larger than the theoretical capacity (288 mA h g^{-1}) of the present NiO/AB electrode with the NiO content of 44 wt%. It is considered that several reactions other than the

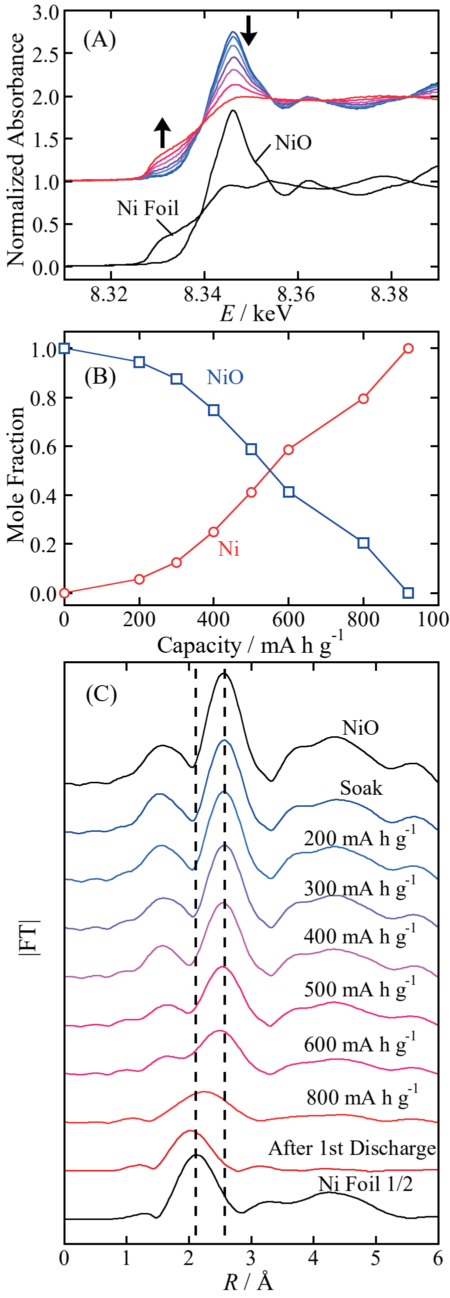

Fig. 2 Ni K-edge XANES spectra of the NiO/AB electrode for various states during the first discharge process (A), the composition of the Ni species versus capacity (B), and the Fourier transform functions of the EXAFS part (C).

reduction of NiO are proceeding at the same time. The similar trend is observed in the change of the Fourier transform function of the extended X-ray absorption fine structure (EXAFS) part shown in Fig. 2(C). While the peak pattern similar to NiO was almost maintained up to 300 mA h g^{-1}, it shifted to that corresponding to Ni(0) as the discharge progresses further. The main peak position of the final state was in agreement with that of Ni foil, indicating the generation of Ni(0) particles.

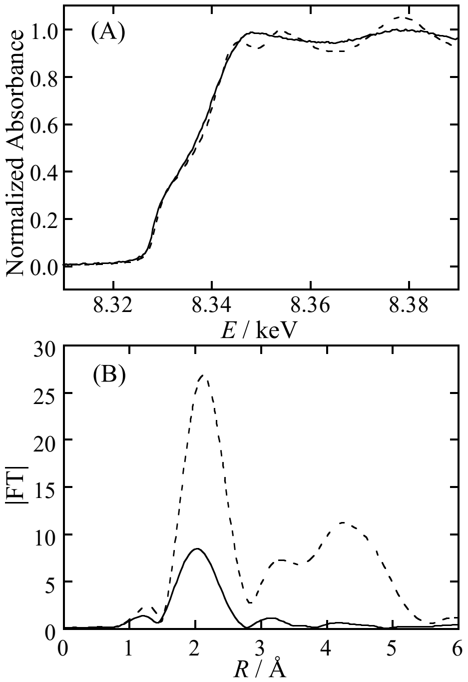

Fig. 3 Ni K-edge XANES spectra (A) and the Fourier transform functions (B) of the fully discharged electrode (solid line) and Ni foil (dashed line).

In Fig. 3, the XANES spectrum and the Fourier transform function for fully discharged electrode are compared with those for Ni foil. The XANES spectra showed the same edge energy, however, the spectral shape was apparently different. The spectral structure on the higher energy side of the absorption edge was smoothed for the discharged electrode, suggesting the reduction of the Ni(0) particle size [13,14]. Because the interatomic distance of the nearest-neighboring Ni–Ni interaction was consistent in two samples, the reduced Ni(0) species was generated in the fully discharged electrode. The low peak height clearly indicates that the Ni(0) particle size is remarkably small. The structure parameters for the Ni–Ni interaction determined by

Table 1 Structure parameters for the nearest-neighboring Ni–Ni interaction.[a]

sample	N	R / Å	σ^2 / 10^{-3} Å^2
Ni foil	12 (fixed)	2.48 ± 0.01	6.7 ± 0.5
electrode	6.6 ± 0.8	2.44 ± 0.01	12.0 ± 1.0

[a] The amplitude reduction factor S_0^2 was determined to 0.93 for the analysis of Ni foil, and the value was fixed in the analysis for the discharged electrode.

the EXAFS analysis for Ni foil and the fully discharged electrode are given in Table 1. The particle size of about 1 nm is estimated from the small coordination number of 6.6 ± 0.8 for the fully discharged electrode [15], while the crystallite size of the synthesized NiO/AB powder is 13 nm estimated by the XRD pattern. The XAFS analyses for the fully discharged electrode have revealed that the Ni particle cracks when the oxide ion is removed from NiO driven by the reduction of the Ni(II) center.

The Ni $L_{2,3}$-edge XANES spectra measured in the PEY and PFY modes are shown in Fig. 4 for the disassembled electrodes during the first discharge process. No obvious difference in spectral shape was seen in both mode until 200 mA h g^{-1}, and the spectral shape was consistent with that of NiO. Then, the main peak at the L_3-edge was diminished at the discharge capacity above 400 mA h g^{-1}. Because the final spectrum showed the shape characteristic of metallic Ni [16], the reduction of NiO to Ni(0) was also supported by the Ni $L_{2,3}$-edge XAFS analysis. The PEY spectra at the Ni $L_{2,3}$-edge represent the chemical state of the particle surface, and the results are consistent with the bulk information measured at the Ni K-edge. It is thus concluded that the reduction of the Ni species proceeds simultaneously at the surface of and inside the particle.

Figure 5 shows the O K-edge XANES spectra measured in the TEY and PFY mode for the disassembled electrodes during the first discharge process. The spectra of the pristine and soaked electrode were identical to that of NiO for both modes, indicating that there was no oxygen-containing compound other than NiO in the electrode at the beginning of the first discharge process. A new peak appeared at 533 eV during the early discharge process up to 200 mA h g^{-1}, and this peak was observed in both spectra measured in different modes. The peak energy corresponds to that of Li_2CO_3, as shown in Fig. 5, which can be generated by the reductive decomposition of electrolyte solvent and is expected to be a component of SEI. The formation of carbonate ion requires the electrons, and thus it is considered that the initial reduction currents up to *ca.* 300 mA h g^{-1} are consumed to generate carbonate ions, not to reduce NiO. This may mean that the formation of Li_2CO_3 is required to facilitate the reduction of NiO. Because the stabilization of oxide ions is essential to reduce NiO, it is reasonable that an ionic compound containing Li^+, such as Li_2CO_3, must be present around the NiO particle. It is then considered that Li_2O generated with the progress of the reduction from NiO to Ni(0) contribute to be reducing the particle size of the Ni species.

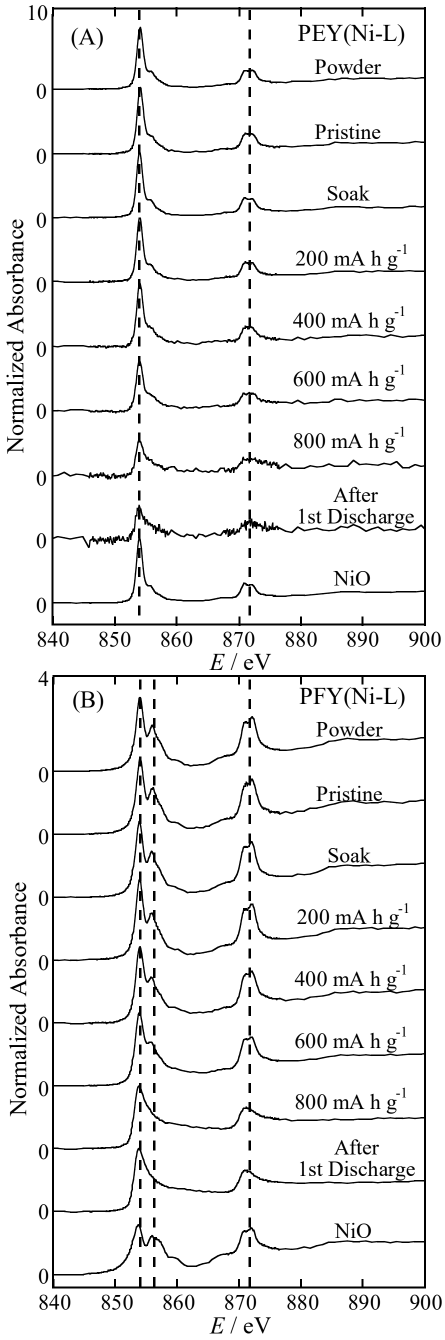

Fig. 4 Ni $L_{2,3}$-edge XANES spectra measured in the PEY (A) and PFY (B) mode for the disassembled electrodes at various states during the first discharge process.

The observed O K-edge XANES spectra are shown in Fig. 6 without the normalization procedure of the edge jump. The overall absorbance increases as the discharge progress, indicating that Li_2CO_3 is produced and deposited in the NiO/AB electrode as SEI. Then, the spectrum derived from NiO was hidden by the contribution of Li_2CO_3 in the normalized XANES spectra at the initial stage of the discharge process up to 200 mA h g^{-1} (see Fig. 5), although NiO still existed at that time. Because the spectrum of Li_2CO_3 continuously increases until the

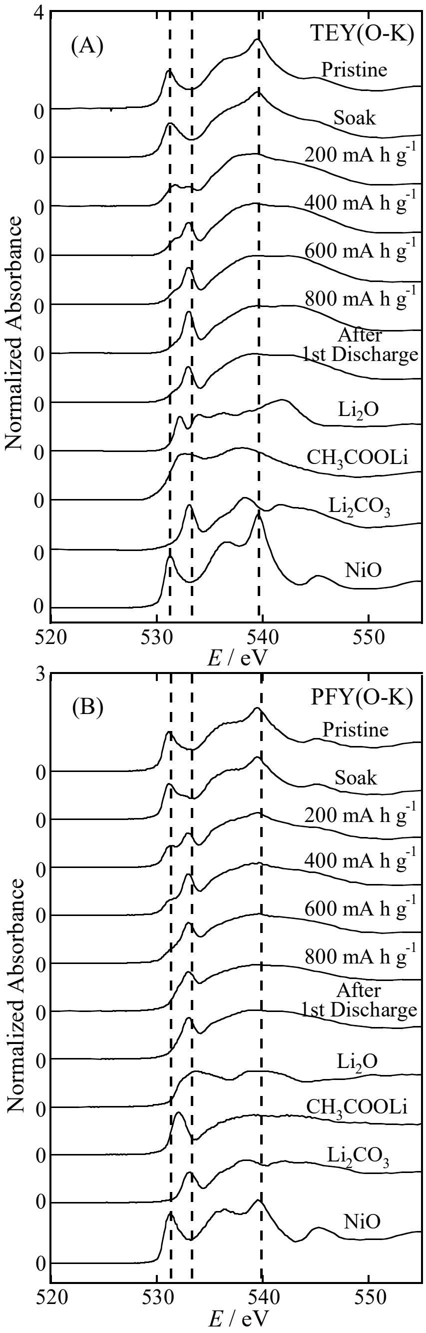

Fig. 5 O K-edge XANES spectra measured in the TEY (A) and PFY (B) mode for the disassembled electrodes at various states during the first discharge process.

end of the discharge process, it is found that the formation of SEI is continued throughout the first discharge process, leading to an extraordinary large discharge capacity. The minute Ni(0) particles are thus produced in the electrode and are surrounded by Li_2O and ionic compounds containing Li^+, such as Li_2CO_3. Once this state is formed, as shown in Fig. 1, the subsequent redox reaction of the NiO/Ni pair is considered to proceed reversibly.

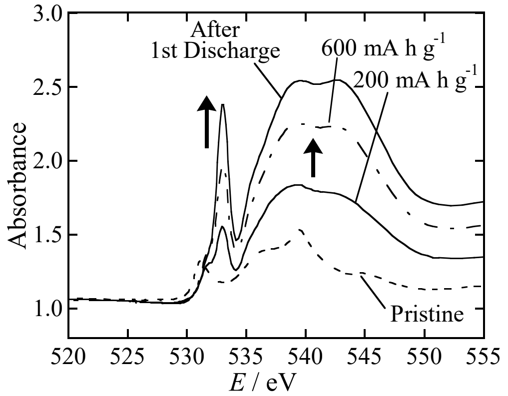

Fig. 6 O K-edge XANES spectra measured in the TEY mode for the disassembled electrodes at various states during the first discharge process without the normalization procedure of the edge jump.

4. Conclusion

In this study, the first discharge process of the NiO/AB electrode was analyzed by the XAFS measurements at the K- and $L_{2,3}$-edges of Ni and at K-edge of O. It is clarified that the formation of Li_2CO_3 as SEI by the reductive decomposition of the electrolyte solvent proceeds prior to the reduction of NiO. The Li^+ ion present in SEI can stabilize the oxide ions released from NiO, and then the NiO particles are reduced to Ni(0) accompanied by the reduction of their particle size and the production of Li_2O. These results indicate that the generation and preservation of small Ni particles embedded in SEI containing Li^+ is a key factor for the reversible cycle of conversion reactions in rechargeable batteries.

Acknowledgement

The XAFS measurements at the Photon Factory (KEK) were performed under the approval of the Photon Factory Program Advisory Committee (Proposal No. 2019G649).

References

[1] T. M. Paronyan, A. K. Thapa, A. Sherehiy, J. B. Jasinski, and J. S. D. Jangam, *ECS Trans.*, **2017**, *77*, 311.

[2] Z. Yao, S. Kim, M. Aykol, Q. Li, J. Wu, J. He, and C. Wolverton, *Chem. Mater.*, **2017**, *29*, 9011.

[3] I. Lahiri, S.-W. Oh, J. Y. Hwang, S. Cho, Y.-K. Sun, R. Banerjee, and W. Choi, *ACS Nano,* **2010**, *4*, 3440.

[4] S. Laruelle, S. Grugeon, P. Poizot, M. Dolle, L. Dupont, and J-M. Tarascon, *J. Electrochem. Soc.*, **2002**, *149*, A627.

[5] P. Polzot, S. Laruelle, S. Grugeon, L. Dupont, and J-M. Tarascon, *Nature*, **2000**, *407*, 496.

[6] X. Liu, S. W. Or, C. Jin, Y. Lv, C. Feng, and Y.

Sun, *Carbon*, **2013**, *60*, 215.
[7] K. Xu, G. V. Zhuang, J. L. Allen, U. Lee, S. S. Zhang, P. N. Ross, Jr., and T. R. Jow, *J. Phys. Chem. B*, **2006**, *110*, 7708.
[8] M. Nie, D. Chalasani, D. P. Abraham, Y. Chen, A. Bose, and B. L. Lucht, *J. Phys. Chem. C*, **2013**, *117*, 1257.
[9] P. Guan, L. Liu, and X. Lin, *J. Electrochem. Soc.*, **2015**, *162*, A1798.
[10] V. A. Agubra and J. W. Fergus, *J. Power Sources*, **2014**, *268*, 153.
[11] P. Arora, R. E. White, and M. Doyle, *J. Electrochem. Soc.*, **1998**, *145*, 3647.
[12] M.-Y. Cheng, Y.-S. Ye, T.-M. Chiu, C.-J. Pan, and B.-J. Hwang, *J. Power Sources,* **2014**, *253*, 27.
[13] Y. Yamamoto, S. Yamashita, N. Afiza, M. Katayama, and Y. Inada, *J. Phys. Conf. Ser.*, **2016**, *712*, 23.
[14] N. Afiza, Y. Yamamoto, K. Maruyama, K. Nakamura, S. Yamashita, M. Katayama, and Y. Inada, *Adv. X-ray Chem. Anal.*, **2016**, *47*, 301.
[15] Y. Yamamoto, A. Suzuki, N. Tsutsumi, M. Katagiri, S. Yamashita, Y. Niwa, M. Katayama, and Y. Inada, *J. Solid State Chem.*, **2018**, *258*, 264.
[16] W.-T. Chen, A. Chan, D. Sun-Waterhouse, T. Moriga, H. Idriss, and G. I. N. Waterhouse, *J. Catal.*, **2015**, *326*, 43.